Electrochemically Triggered Au Nanoparticles "Sponges" for the Controlled Uptake and Release of a Photoisomerizable Dithienylethene Guest Substrate

Junji Zhang,[†,‡] Michael Riskin,[†] Ronit Freeman,[†] Ran Tel-Vered,[†] Dora Balogh,[†] He Tian,[‡,*] and Itamar Willner[†,*]

[†]Institute of Chemistry and the Center for Nanoscience and Nanotechnology, The Hebrew University of Jerusalem, Jerusalem, 91904, Israel and [‡]Laboratory for Advanced Materials, Institute of Fine Chemicals, East China University of Science and Technology, Shanghai, 200237, P. R. China

The preparation of signal-triggered modified surfaces is one of the challenging topics in material science.[1] Different applications of monolayer- or thin film-functionalized surfaces, such as selective sensing,[2] controlled release and delivery of drugs,[3] controlled wettability,[4] charge transport at electrode surfaces,[5] and others,[6] were suggested. Different external stimuli, such as electrical,[7] optical,[8] pH,[9] thermal,[10] magnetic,[11] or chemical[12] stimuli, were used to control the properties and functions of the modified surfaces. Imprinted polymers, assembled as thin films on surfaces, provide "smart" matrices for selective sensing and separation.[13] Recently, we reported on the imprinting of specific molecular recognition sites in electropolymerized bis-aniline-cross-linked Au nanoparticles (NPs) composites associated with electrodes. We demonstrated that the electropolymerization of thioaniline-functionalized Au NPs in the presence of electron acceptors, or negatively charged substrates (or structural analogues to the substrates), led to the formation of imprinted sites through donor−acceptor or electrostatic affinity interactions, respectively.[14] Similarly, the cofunctionalization of the thioaniline-modified Au NPs with specific ligands enabled the imprinting of molecular recognition sites into the Au NPs matrices by electrostatic or ligand-substrate interactions.[15] These imprinting procedures were implemented to develop selective sensing matrices for explosives, for example, TNT,[16] RDX,[17] PETEN,[18] and EGDN,[18] and the detection of saccharides[19]

ABSTRACT 1,2-Di(2-methyl-5-(*N*-methylpyridinium)-thien-3-yl)-cyclopentene undergoes a reversible photoisomerization between open and closed states. The closed isomer state exhibits electron acceptor properties, whereas its irradiation using visible light ($\lambda > 530$ nm) yields the open state that lacks electron acceptor features. The electropolymerization of thioaniline-functionalized Au nanoparticles (NPs) in the presence of the closed photoisomer state yields a molecularly imprinted Au NPs matrix, cross-linked by redox-active bis-aniline π-donor bridges. The closed isomer is stabilized in the imprinted sites of the bis-aniline-bridged Au NPs composite by donor−acceptor interactions. The electrochemical oxidation of the bis-aniline bridging units to the quinoid acceptor state leads to imprinted sites that lack affinity interactions for the binding of the closed state to the matrix, leading to the release of the closed photoisomer to the electrolyte solution. By the cyclic reduction and oxidation of the bridging units to the bis-aniline and quinoid states, the reversible electrochemically controlled uptake and release of the closed photoisomer is demonstrated. The quantitative uptake and release of the closed isomer to and from the imprinted Au NPs composites is followed by application of CdSe/ZnS quantum dots as auxiliary probes. Similarly, by the reversible photochemical isomerization of the closed substrate to the open substrate ($\lambda > 530$ nm) and the reversible photoizomerization of the open substrate to the closed state ($\lambda = 302$ nm), the cyclic photonic uptake and release of the closed substrate to and from the imprinted Au NPs matrix are demonstrated. Finally, we demonstrate that the electrochemically stimulated uptake and release of the closed substrate to and from the imprinted Au NPs composite controls the wettability of the resulting surface.

KEYWORDS: Au nanoparticles · electrochemistry · photochemistry · wettability · switch

or antibiotics.[20] The unique features of the molecularly imprinted Au NPs composite are as follows: (i) The imprinted sites exhibit high affinity for the selective binding of the imprinted substrates. (ii) The localized plasmon associated with the Au NPs results in its coupling with the surface plasmon wave associated with the thin metal films deposited on the solid supports. This electronic coupling leads to shifts in the resonance
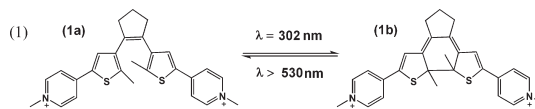
spectrum of the surface wave. Thus, changes in the dielectric properties in the composite, as a result of binding or dissociation of a substrate to and from the molecular recognition sites, are amplified through the electronic coupling of the localized NPs plasmon with the surface plasmon wave. (iii) The bis-aniline units, bridging the Au NPs, exhibit a quasi-reversible redox wave that enables the potential-induced cyclic transformation of the bridging units from the π-donor bisaniline state to the π-acceptor quinoid state, and back. (iv) The Au NPs can be modified by functional coadditives in the capping layer leading to multifunctional NPs composites. For example, thiolated nitrospiropyran photoisomerizable units were assembled on an imprinted, cross-linked, Au NPs composite to yield an electrochemically/photochemically triggered matrix.[21] The unique properties of the imprinted Au NPs matrices were implemented to develop electrochemically triggered "sponges" for the selective electrically triggered uptake and release of the imprinted substrates.[22] Also, the electrochemically switched uptake and release of the imprinted substrates led to the controlled wettability of surfaces.[21,23] The imprinted bis-aniline-cross-linked Au NPs composites, modified with nitrospiropyran photoisomerizable units, were used as an electrochemically and/or photochemically activated "sponge" that enabled the stimuli-regulated uptake or release of a zwitterionic electron acceptor to/from the Au NPs matrix, and the control of the wettability of the surface.[21] Here we wish to report on the preparation of an imprinted Au NPs composite for the selective association of a photoisomerizable substrate exhibiting electron acceptor properties. We demonstrate the electrochemical or photochemical uptake/release of the substrate by the imprinted composite and the subsequent control of the wettability of the surface. In a contrast to the previous study[21] that implemented imprinted Au NPs composites modified with photoisomerizable nitromerocyanine units and bis-aniline π-donor cross-linking bridges for the electrochemical and photochemical controlled uptake and release of a zwitterionic electron acceptor, the present study demonstrates the use of the electroactive imprinted Au NPs matrix for the controlled uptake and release of a photoisomerizable substrate, exhibiting electron acceptor properties in one of the photoisomer states.

RESULTS AND DISCUSSION

The molecule 1,2-di(2-methyl-5-(N-methylpyridinium)-thien-3-yl)-cyclopentene, **1a**, undergoes a photochemical 6π-electrocyclic cyclization upon irradiation, $\lambda = 302$ nm, to form the photoisomer **1b**. The irradiation of **1b** with visible light, $\lambda > 530$ nm, results in the back isomerization to **1a**, eq 1. The planar structure of the isomer **1b** and the delocalization across the pyridinium sites, suggest that the isomer **1b** exhibits

acceptor properties similar to other conjugated bipyridinium salts. Accordingly, we anticipated that the photoisomer **1b** could act as a substrate in the preparation of an electrochemically/photochemically triggered uptake/release system, as outlined in Figure 1.

Au NPs (*ca.* 4 nm) functionalized with thioaniline electropolymerizable units, (**2**), and mercaptoethane sulfonic acid, (**3**), as a stabilizing cocomponent in the capping layer, were electropolymerized in the presence of **1b**, 2.5 mM, on a thioaniline monolayer-functionalized Au surface. The electropolymerization was performed by the application of 80 cyclic voltammetry scans in the range of -0.3 V to $+0.8$ V *vs* SCE. The imprinted substrate was rinsed-off from the resulting bis-aniline-bridged Au NPs composite to yield the **1b**-imprinted Au NPs matrix (Figure 1A). A similar electropolymerization process was used to polymerize the functionalized Au NPs in the absence of **1b**, to yield the nonimprinted bis-aniline-cross-linked Au NPs composite. The bis-aniline units, bridging the Au NPs, exhibit a quasi-reversible redox wave at *ca.* $E^{\circ\prime} = 0.05$ V *vs* Ag quasi-reference electrode (Ag QRE) at pH = 7.2. This redox process transforms the bis-aniline donor bridges to the quinoid acceptor state, and back (Figure 1A, eq 2). Microgravimetric quartz crystal microbalance (QCM) measurements indicated that the mass associated with the Au NPs composite corresponded to *ca.* 1.9×10^{-5} g cm^{-2}, a value that translates to a surface coverage of *ca.* 4×10^{13} Au NPs cm^{-2}. Figure 2A, curve a, shows the surface plasmon resonance (SPR) spectrum of the thioaniline-modified Au surface, whereas curve b depicts the SPR spectrum of the surface after the electropolymerization of the Au NPs in the presence of **1b**. The shift in the SPR spectrum indicates that the Au surface was modified with the Au NPs composite. Figure 2A, curve c, shows the SPR spectrum of the modified surface after rinsing of the imprinting substrate, **1b**. The resulting SPR spectrum shows a lower value for the minimum reflectivity angle, which is attributed to the changes in the dielectric properties of the composite film as a result of the elimination of the imprinting substrate **1b**. Indeed, further treatment of the vacant imprinted Au NPs matrix with **1b** results in the SPR spectrum shown in curve d, which is almost identical to the spectrum obtained upon the electrosynthesis of the imprinted matrix. The subsequent removal of **1b** from the modified surface yields, again, the vacant matrix, as demonstrated in curve e. The shifts in the SPR spectrum are, thus, attributed to the dielectric changes occurring upon the binding, or release, of **1b** to or from the imprinted Au NPs composite. These results imply that the reflectance changes of the SPR spectra may qualitatively report the binding
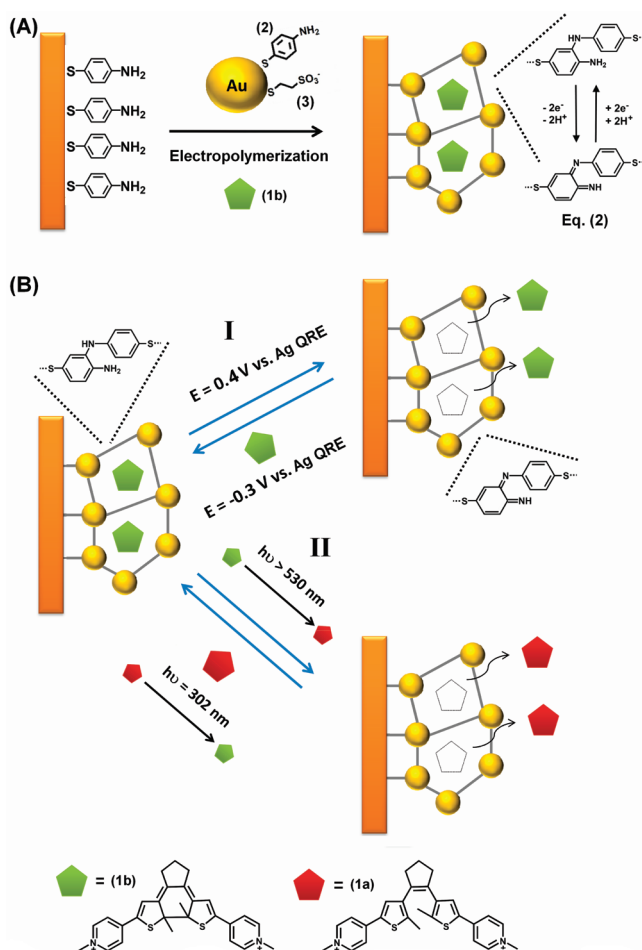
Figure 1. (A) Schematic presentation of the electropolymerization of the bis-aniline-cross-linked Au NPs composite and the imprinting of the π-acceptor molecule 1b. (B) Electro-stimulated (I) and photostimulated (II) uptake and release of 1b using the imprinted bis-aniline-cross-linked Au NPs composite.

and dissociation of **1b** to, and from, the Au NPs film. Figure 2B, curve a, shows the reflectance changes of the imprinted Au NPs composite upon interaction with different concentrations of **1b** for 20 min. For comparison, curve b depicts the reflectance changes associated with the nonimprinted Au NPs composite. While the nonimprinted Au NPs composite reveals minute reflectance changes, indicating low binding capacities for **1b**, the imprinted Au NPs matrix reveals substantially higher values, implying higher affinities for the association of **1b**. The reflectance changes level off at a concentration of **1b** that corresponds to *ca.* 1 μM, and this is attributed to the saturation of the imprinted sites associated with the Au NPs composite with **1b**. Assuming a Langmuir-type binding of **1b** to the imprinted sites, we calculated, from Figure 2B, curve a, the association constant of **1b** to the imprinted sites, $K_a = 1.6 \times 10^8$ M^{-1} (see Figure S1, Supporting Information). Realizing that the affinity of **1b** to the imprinted sites originates from cooperative π-donor$-$acceptor interactions between **1b** and the donor bis-aniline units, due to the steric fit between **1b** and the imprinted molecular contours, we examined the effect of the

applied potential on the binding of **1b** to the imprinted sites. Figure 2C, curve a, shows the reflectance changes (ΔR) measured for the Au NPs composite in the presence of **1b**, 20 nM, at different applied potentials. Evidently, at positive potentials the reflectance changes are very low, and even slightly negative, and as the potential is shifted negatively, the reflectance changes intensify. Also, the ΔR values demonstrate a sharp increase at *ca.* $E = 0.05$ V vs Ag QRE, and level off to a constant value at *ca.* $E = -0.1$ V. The effect of potential on the reflectance changes in the presence of **1b** is attributed to the redox state of the bridging units. The sharp changes in the ΔR values are observed at $E = 0.05$ V, the redox potential of the redox-active bis-aniline bridging units. That is, at more positive potentials, the bridging units exist in the quinoid acceptor state that lacks affinity for **1b** and, thus, the reflectance changes are small. At $E < 0.05$ V the bis-aniline bridges are formed, and the association of **1b** to the high affinity binding sites leads to enhanced reflectance changes. As the potential is shifted to more negative values, the reflectance changes reach a constant value, consistent with the transformation of all bridges into the bis-aniline state and the saturation of the bridging sites
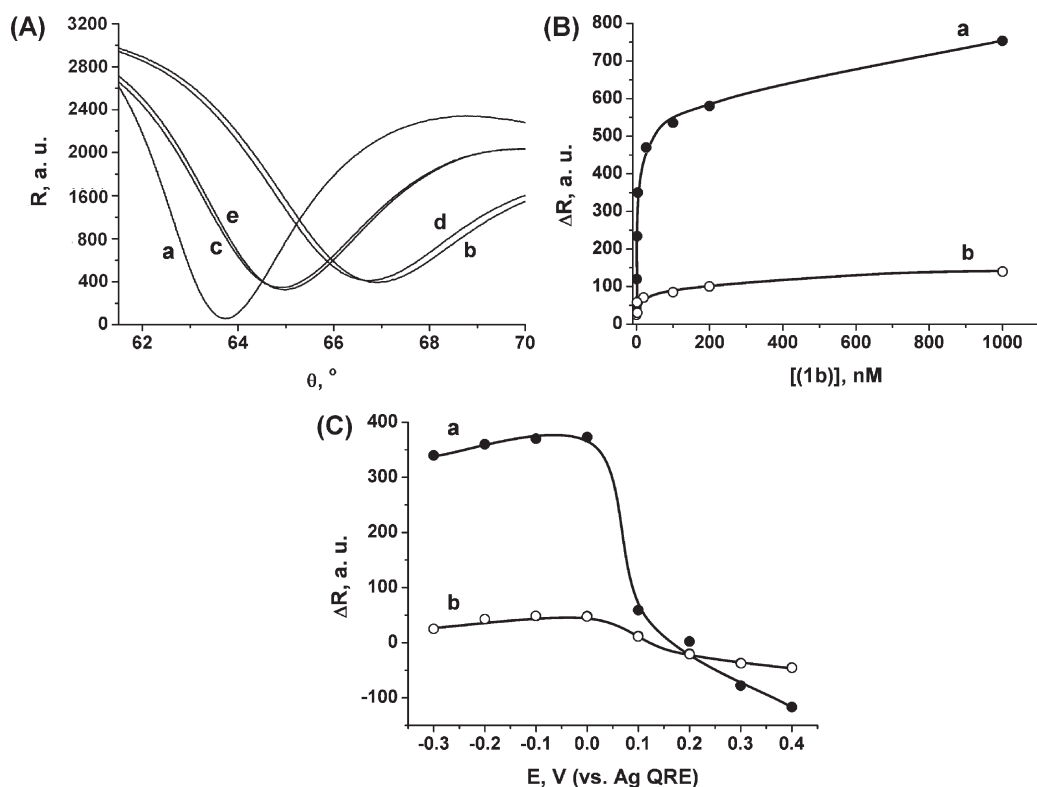
Figure 2. (A) SPR curves corresponding to (a) the thioaniline-modified Au surface before electropolymerization with the thioaniline-functionalized Au NPs, (b) the bis-aniline-cross-linked Au NPs composite electropolymerized on the Au surface in the presence of 1b, 2.5 mM, (c) the 1b-imprinted bis-aniline-cross-linked Au NPs matrix, following the removal of the imprint molecule, (d) the 1b-imprinted bis-aniline-cross-linked Au NPs matrix, following its interaction with 1b, 1 μM, (e) the 1b-imprinted bis-aniline-cross-linked Au NPs matrix, following the removal of the 1b molecule. (B) Calibration curves corresponding to the changes in the reflectance intensities, at a constant angle $\theta = 63.5°$, upon the interaction of variable concentrations of 1b, for 20 min, with (a) the 1b-imprinted and (b) the nonimprinted matrices. (C) Effect of applied potential on the reflectance changes, at $\theta = 63.5°$, of the bis-aniline-cross-linked Au NPs composite, upon interacting 1b, 20 nM, with (a) the imprinted composite and (b) the nonimprinted composite. All measurements were performed in 0.1 M HEPES buffer solution, pH = 7.2.

with **1b**. These results indicate that the applied potential may, indeed, control the association or dissociation of **1b** to, or from, the imprinted Au NPs matrix, and that SPR may be used as a physical readout signal to follow these processes. The effect of applied potential on the Au NPs matrix in the absence of **1b** is shown in Figure 2C, curve b. In this case, only small reflectance changes are induced by the potential due to the lower affinity of **1b** to the nonimprinted matrix.

Figure 1B, path I shows the schematic potential-induced uptake and release of **1b** to and from the imprinted Au NPs matrix. The reduction of the bridges, at $E = -0.3$ V, to the bis-aniline state results in the association of **1b** to the imprinted sites, whereas the oxidation of the bridges to the quinoid state, at $E = +0.4$ V, leads to the dissociation, and release, of **1b** from the composite. Figure 3A demonstrates the cyclic uptake and release of **1b** by the **1b**-imprinted surface. Application of the negative potential results in a time-dependent increase in the reflectance, implying that **1b** binds to the imprinted sites. Reversing the potential to the positive value, leads, then, to the time-dependent decrease of the reflectance changes, indicating that **1b** is released from the imprinted matrix.

We, then, examined the possibility to control the binding and dissociation of **1b** to and from the imprinted matrix using light, by exploiting the fact that **1a** exhibits reversible photoisomerizable properties, eq 1. While **1a** lacks electron acceptor properties, the photoisomer **1b** indeed reveals such features. We find that the **1b**-imprinted Au NPs composite demonstrates selective association properties and the photoisomer **1a** does not bind to the matrix, thus leading to lower reflectance changes. Accordingly, we examined the possibility to control the association and dissociation of **1b** to and from the surface by light (Figure 1B, path II). Figure 3B, region I, shows two photochemical uptake and release cycles of **1b** to and from the **1b**-imprinted Au NPs matrix. The uptake of the photoisomer **1b** by the bis-aniline-bridged Au NPs composite is relatively fast, and it is followed by an increase in the reflectance. Photoisomerization of **1b** in the solution, $\lambda > 530$ nm, yields **1a**, and the process is followed by a slow decrease in the reflectance of the system, indicating the slow release of the substrate associated with the composite. Evidently, a subsequent rephotoisomerization of **1a** to **1b** leads to the rapid uptake of the imprinted substrate by the imprinted sites, and the secondary photoisomerization
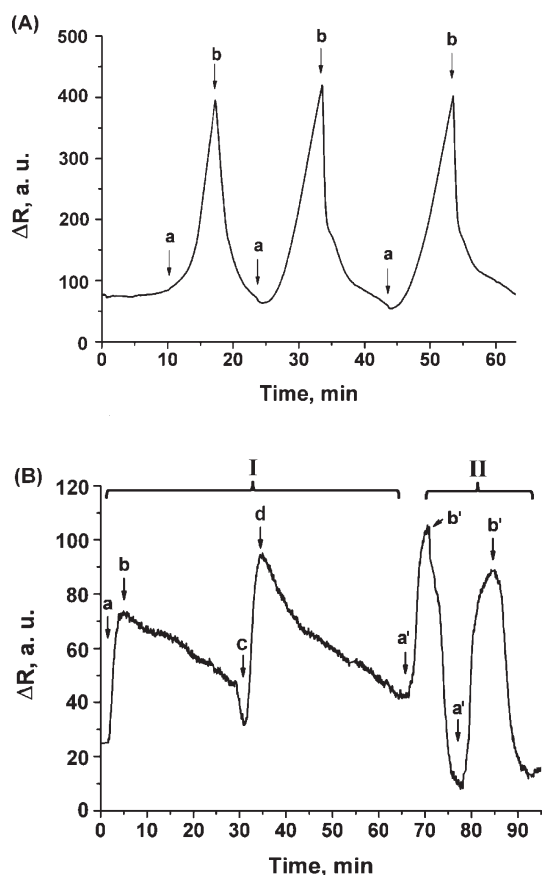
Figure 3. (A) Time-dependent reflectance changes corresponding to the cyclic electrostimulated uptake and release of 1b, 20 nM, by the 1b-imprinted bis-aniline-cross-linked Au NPs composite-modified Au electrode, upon the application of cyclic potentials on the electrode: (a) $E = -0.3$ V (vs Ag QRE), and (b) $E = 0.4$ V. (B) Time-dependent reflectance changes corresponding to the uptake and release of 1b, 5 nM, by the composite in panel A. Region I: (a) Interaction of the composite with the 1b solution after the photoisomerization of 1a for 10 min at $\lambda = 302$ nm, and the application of $E = -0.3$ V on the electrode for 10 min, (b) illumination of the composite and the solution in (a) by visible light, $\lambda > 530$ nm, (c) interaction of the composite in (b) with the solution, after its illumination by UV light, $\lambda = 302$ nm, for 10 min, (d) illumination of the composite in (c) by visible light, $\lambda > 530$ nm. Region (II): (a') Interaction of the composite with the 1b solution after the application of $E = -0.3$ V on the electrode for 10 min, and (b') interaction of the composite with the 1b solution after the application of $E = 0.4$ V on the electrode for 10 min. All measurements were performed in a 0.1 M HEPES buffer solution, pH = 7.2.

of 1b to 1a leads to the cyclic release of the substrate from the Au NPs matrix. It should be noted that in contrast to the fast electrochemically driven uptake and release of 1b to and from the matrix, the photochemical release of 1b from the matrix is slower. Two major reasons may contribute to this difference: (i) In the electrochemically driven process the electrode is biased at a positive potential, $E = +0.4$ V, that results in the quinoid states. The release of 1b from the matrix does not only originate from the fact that the bridging units are transformed to the acceptor state, but it is also assisted by electrostatic repulsion by the positively charged electrode. (ii) In the photochemically induced release we photoisomerize 1b to 1a in solution,

and make use of the fact that the content of 1b associated with the matrix is low, as compared to the content of 1b in the electrolyte solution (vide infra). As a result, the release of 1b from the matrix is controlled by the need to establish an equilibrium state due to the depletion of 1b in the solution through photoisomerization to 1a. This process is relatively slow, particularly since the bridging units are present in the π-donor bis-aniline state. The photochemically controlled uptake and release of 1b by the 1b-imprinted composite was, then, followed by two electrochemically driven uptake/release cycles of 1b (Figure 3B, region II).

The discussion until now demonstrated the process of imprinting molecular recognition sites for the photoisomer 1b in a Au NPs composite, and the implementation of SPR spectroscopy to follow the electrochemically or photochemically triggered uptake and release of 1b to/from the imprinted matrix. We directed our research, however, to an effort of evaluating quantitatively the activity of the Au NPs composite as an electrochemically driven "sponge". Toward this goal, we used CdSe/ZnS quantum dots (QDs) as an auxiliary label that follows the concentration of 1b in the electrolyte solution, in the presence of the electroactive Au NPs "sponge". We have modified two different sized CdSe/ZnS QDs with mercaptopropionic acid, which allowed us to concentrate the positively charged electron acceptor 1b at the QDs surface, thus enhancing their quenching by the acceptor units, Figure 4A. Evidently, the luminescence quenching of the smaller QDs ($\lambda_{em} = 490$ nm) by 1b is inefficient (see Figure S2A, Supporting Information). On the other hand, the luminescence quenching of the larger QDs ($\lambda_{em} = 620$ nm) proceeds effectively, (Figure S2B, Supporting Information). To account for this difference, we refer to the absorption spectrum of 1b that demonstrates an absorbance band that overlaps the luminescence of the larger-sized CdSe/ZnS QDs, but lacks significant overlap with the luminescence spectrum of the smaller QDs (Figure S3, Supporting Information). Thus, we conclude that 1b acts as an inefficient quencher for the QDs by an electron transfer quenching mechanism, yet it acts as an effective quencher of the larger QDs by a fluorescence resonance energy transfer (FRET) mechanism. The calibration curve showing the luminescence intensities of the larger-sized QDs at different concentrations of 1b is shown in Figure 4B. This calibration curve is used to follow quantitatively the electrochemically triggered uptake and release of 1b to and from the 1b-imprinted Au NPs composite, using the QDs as an auxiliary luminescence probe. The interaction of the 1b solution with the electrode, modified with the imprinted Au NPs composite, followed by biasing the electrode at $E = -0.3$ V, results in the uptake of 1b by the composite. Analysis of the electrolyte solution through the addition of the QDs reveals a high luminescence spectrum, Figure 4C, curve a,
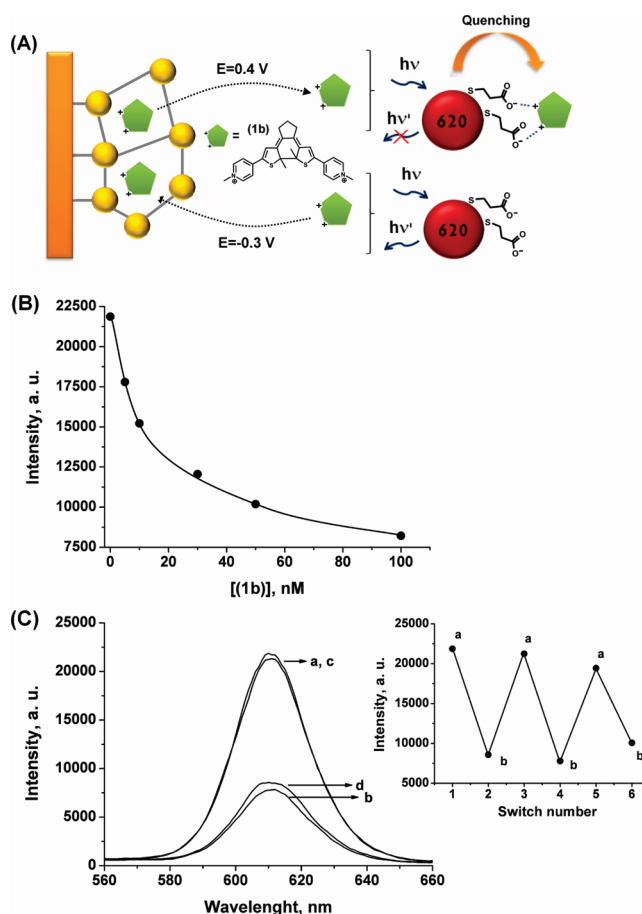
Figure 4. (A) Photonic imaging of the electrochemical uptake and release of 1b to and from the 1b-imprinted bis-aniline-cross-linked Au NPs composite using CdSe/ZnS QDs as auxiliary optical labels. (B) Calibration curve corresponding to the fluorescence intensity of CdSe/ZnS QDs (λ_{em} = 620 nm), 10^{-10} M, in a HEPES buffer solution (0.1 M, pH = 7.2), that contains different concentrations of 1b. Excitation wavelength: λ_{ex} = 430 nm. (C) Emission spectra of CdSe/ZnS QDs (λ_{em} = 620 nm), 10^{-10} M, in a HEPES buffer solution (0.1 M, pH = 7.2) that contains 1b, 100 nM, following the sequential application of (a) E = −0.3 V (vs Ag QRE), (b) E = 0.4 V, (c) E = −0.3 V, and (d) E = 0.4 V, for 10 min. Inset: The maximal fluorescence values, at λ = 620 nm, measured following the cyclic application of the potential triggers.

consistent with the depletion of **1b** from the electrolyte solution through its uptake by the imprinted Au NPs "sponge". The subsequent release of **1b** from the Au NPs-functionalized electrode, under an applied bias potential of E = +0.4 V, followed by the analysis of the content of **1b** in the electrolyte solution with the luminescent QDs, reveals a low luminescence spectrum, Figure 4C, curve b, reflecting that **1b** is released from the composite. In turn, recharging the electrode with the electrolyte solution that includes **1b**, while biasing the electrode at E = −0.3 V, indicates that the content of **1b** in the electrolyte solution is depleted through the association of **1b** with the "sponge", as evidenced by the high luminescence of the QDs, Figure 4C, curve c. The subsequent release of **1b** from the matrix is depicted in curve d. This process of probing the uptake/release of **1b** by the use of the QDs as auxiliary luminescent probe can be further cycled, Figure 4C, inset. It should be noted that the nonimprinted Au NPs composite did not show any detectable uptake/release of **1b** through the quenching of the QDs. From the luminescence changes of the QDs

upon the electrochemically stimulated uptake of **1b**, and by using the calibration curve shown in Figure 4B, we estimate that *ca*. 1.5 × 10^{-11} mole·cm^{-2} of 1b were linked to the Au NPs "sponge".

The photoisomer **1b** is positively charged, and hence the electrochemical uptake and release of **1b** to and from the Au NPs "sponge" are anticipated to control the wettability of the surface. Figure 5A, panel a, shows an aqueous electrolyte droplet that includes **1b** positioned on the imprinted Au NPs-modified Au surface being subjected to the negative potential of E = −0.3 V. The droplet exhibits a contact angle that corresponds to ϕ = 32.5°, revealing the generation of a hydrophilic surface. By applying the oxidative potential (E = 0.4 V) on the Au NPs-functionalized electrode, the bridging units are transformed to the quinoid state. Under these conditions, the contact angle of the droplet changes to ϕ = 46.7°, Figure 5A, panel b, implying that a surface of enhanced hydrophobicity is generated. By the cyclic application of the negative and positive potentials on the imprinted Au NPs composite, the contact angles are reversibly switched between low
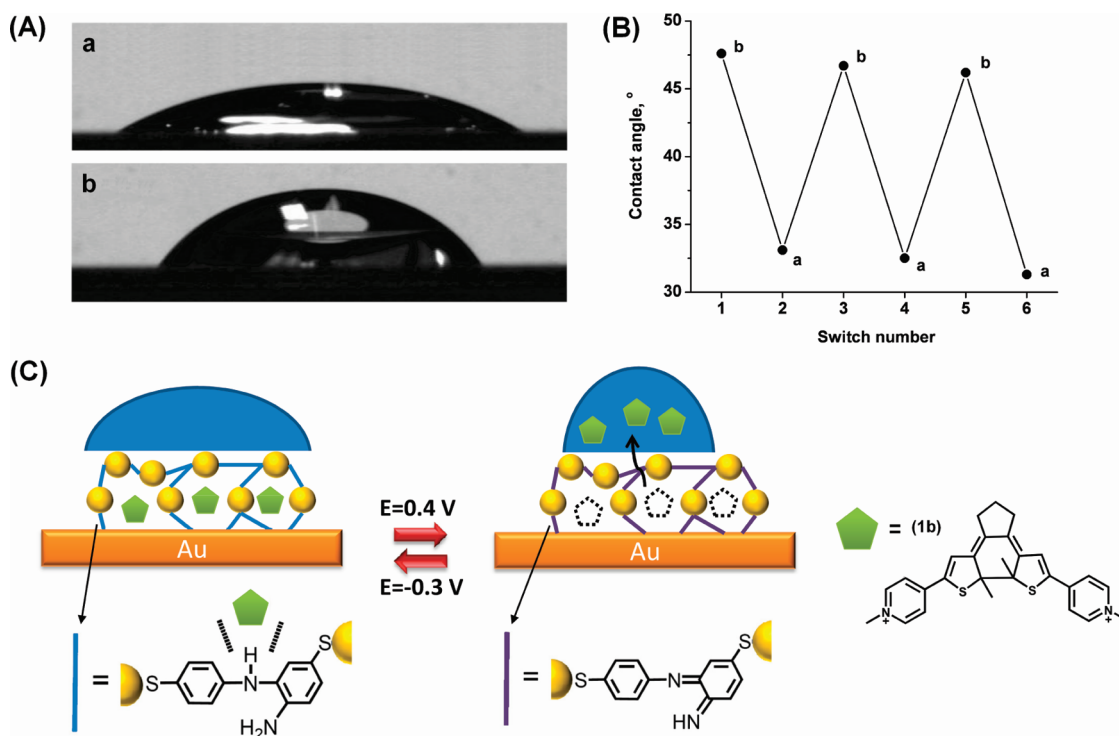
(A)

(B)

(C)

Figure 5. (A) Images showing changes in the contact angle for a droplet containing 1b, 20 nM, on the 1b-imprinted bis-aniline-cross-linked Au NPs electrode, upon the application of (a) a reductive potential pulse, $E = -0.3$ V (vs Ag QRE), for 10 min, (b) an oxidative potential pulse, $E = 0.4$ V, for 10 min. (B) Cyclic electrical switching of the contact angle of the droplet in panel A by the application of (a) $E = -0.3$ V for 10 min, and (b) $E = 0.4$ V for 10 min. (C) Electrostimulated wettability changes by the uptake and release of 1b molecules using the imprinted bis-aniline-cross-linked Au NPs composite. All measurements were performed in a 0.1 M HEPES buffer solution, pH = 7.2.

and high values, respectively, Figure 5B. Control experiments demonstrated that in the presence of **1b**, the nonimprinted Au NPs composite revealed only minute contact angle changes upon applying the reductive or oxidative potentials on the electrode ($\Delta\phi = 3°$). Also, the imprinted Au NPs composite showed minute contact angle changes in the absence of **1b** and upon the application of the negative or positive potentials. These results and the respective control experiments imply that the contact angle changes originate from the potential-induced uptake and release of **1b** to/from the imprinted Au NPs composite, as schematically outlined in Figure 5C. When the imprinted Au NPs composite is biased by the negative potential ($E = -0.3$ V), the potential-induced uptake of **1b** proceeds, resulting in an interface of enhanced hydrophilicity. In turn, when the electrode is subjected to the positive potential ($E = 0.4$ V), the electron acceptor **1b** is released from the composite, resulting in a surface of lower hydrophilicity.

In conclusion, the present study has demonstrated the successful imprint of selective molecular recognition sites for the electrocyclized dithienylethene photoisomer **1b** that exhibits electron acceptor properties. The imprinting process led to the formation of a molecularly imprinted Au NPs composite that revealed selectivity and high binding capacities for the imprinted substrate. The electrochemically triggered uptake and release of **1b** to and from the Au NPs composite has been demonstrated through the cyclic electrochemical reduction and oxidation of the bis-aniline units that bridge the NPs and transform the linker units between the π-donor and the π-acceptor states, respectively. Similarly, the photonic release of **1b** from the Au NPs composite was demonstrated through the photo-isomerization of **1b** to the open photoisomer state, **1a**, that lacks acceptor properties. Finally, the electrochemically triggered uptake and release of **1b** to and from the Au NPs composite led to the cyclic switchable wettability of the surface.

METHODS

Synthesis of 1,2-Di(2-methyl-5-(N-methylpyridinium)-thien-3-yl)-cyclopentene, 1a. 1,2-Di(2-methyl-5-(pyrid-4-yl)-thien-3-yl)cyclopentene (DTEPy) was synthesized according to a previously reported procedure,[24] and characterized by ^{1}H NMR. To synthesize **1a**, 0.1 g (0.24 mmol) of DTEPy, dissolved in 20 mL of dry acetonitrile, was

reacted with 0.075 mL (1.2 mmol) of CH_3I in the dark. The solution was stirred for 24 h at 70 °C. The solvent was then evaporated in vacuum, and the extract was washed with ether. Following filtration, a yellow solid of **1a** was obtained with 90% yield. ^{1}H NMR (400 MHz, CD$_3$OD, 25 °C): d (ppm) 2.10 (s, 6 H), 2.19 (m, 2 H), 2.94 (t, $J = 7.2$, 4 H), 4.35 (s, 6 H), 7.97 (s, 2 H), 8.13 (d, $J = 6.8$, 4 H), 8.75 (d, $J = 7.2$, 4 H).

Nanoparticles and QDs Syntheses. Au nanoparticles functionalized with 2-mercaptoethane sulfonic acid and *p*-aminothiophenol (Au NPs) were prepared by mixing a 10 mL solution containing 197 mg of $HAuCl_4$ in methanol, a 5 mL solution containing 42 mg of mercaptoethane sulfonate, and 8 mg of *p*-aminothiophenol in methanol. The two solutions were stirred in the presence of 2.5 mL of glacial acetic acid on an ice bath for 1 h. Subsequently, 7.5 mL of aqueous solution of 1 M sodium borhydride, $NaBH_4$, was added dropwise, resulting in a dark color solution associated with the presence of the Au NPs. The solution was stirred for 1 additional hour in an ice bath, and then for 14 h at room temperature. The particles were successively washed and centrifuged (twice in each solvent) with methanol, ethanol, and diethyl ether. A mean particle size of *ca.* 4 nm was estimated using TEM. CdSe/ZnS QDs ($\lambda_{em} = 490$ or 620 nm) were precipitated from a toluene solution by the addition of 2 mL of methanol to 0.5 mL of QDs, in toluene, followed by a centrifugation for 5 min at 3000 rpm. The resulting precipitate was dissolved in 1 mL of chloroform, to which 200 μL of mercaptopropionic acid solution (containing 0.142 g mercaptopropionic acid and 40 mg KOH in 2 mL methanol) was added, and the resulting mixture was shaken for 10 min. Subsequently, 1.5 mL of 1 mM aqueous NaOH solution was added to the system, resulting in the transfer of the QDs to the aqueous phase. The QDs solution was, then, separated from the chloroform by centrifugation for 1 min. The excess of mercaptopropionic acid was removed by two successive precipitation steps of the QDs, using NaCl and methanol. The resulting QDs were dissolved in 200 μL of a 10 mM HEPES buffer (pH = 7.4).

Modification of the Electrodes. *p*-Aminothiophenol-functionalized electrodes were prepared by immersing the Au slides for 24 h into a *p*-aminothiophenol ethanolic solution, 50 mM. To prepare the bis-aniline-cross-linked Au NPs composite on the electrode, the surface-tethered *p*-aminothiophenol groups were electropolymerized in a 0.1 M HEPES solution (pH = 7.2) containing 2 mg·mL^{-1} of *p*-aminothiophenol-functionalized Au NPs. The polymerization was performed by the application of 80 potential cycles between $E = -0.3$ and $E = 0.8$ V vs a KCl-saturated calomel electrode (SCE), at a potential scan rate of 100 mV s^{-1}. The resulting films were then washed with the background buffer solution to exclude any residual monomer from the electrode. Similarly, imprinted bis-aniline-cross-linked films were prepared by adding 2.5 mM of the imprint molecule to the Au NPs mixture prior to the electropolymerization process. The extraction of the imprint molecules from the film was carried out by immersing the electrodes overnight in a phosphate buffer solution (0.1 M, pH = 7.4) at room temperature.

Instrumentation. A surface plasmon resonance (SPR) Kretschmann-type spectrometer NanoSPR 321 (NanoSPR devices, USA), with a LED light source, $\lambda = 650$ nm, and a prism refraction index $n = 1.61$, were used. The SPR measurements were performed using a home-built cell, volume 0.2 mL. In the potential-induced measurements, a PC-controlled (Autolab GPES software) potentiostat/galvanostat (μAutolab, type III) was used. In these measurements, a graphite rod ($d = 5$ mm) was used as the counter electrode. Fluorescence measurements were performed using a Cary Eclipse Device (Varian Inc.). Static contact-angle measurements were performed on the modified Au by using a CAM 2000 optical-angle analyzer (KSV Instruments, Finland). A droplet of the HEPES buffer solution (0.1 M, pH = 7.2), approximately 20 μL with diameter of roughly 0.5 cm, was deposited on the surface by using a syringe. The images of the droplets were recorded and each contact angle measurement was repeated at least three times. The reported values represent the average of these results.

Supporting Information Available: The derivation of the association constant for **1b** to the Au NPs matrix, emission spectra of the different QDs in the presence of **1b**, and the absorption spectra of the **1a** and **1b** photoisomers and the QDs. This material is available free of charge *via* the Internet at http://pubs.acs.org.

REFERENCES AND NOTES

1. Nath, N.; Chilkoti, A. Creating "Smart" Surfaces Using Stimuli Responsive Polymers. *Adv. Mater.* **2002**, *14*, 1243–1247.

2. He, X.; Wang, X.; Jin, X.; Zhou, H.; Shi, X.; Chen, G.; Long, Y. Epimeric Monosaccharide-Quinone Hybrids on Gold Electrodes toward the Electrochemical Probing of Specific Carbohydrate-Protein Recognitions. *J. Am. Chem. Soc.* **2011**, *133*, 3649–3657.

3. Knezevic, N.; Trewyn, B.; Lin, V. Light- and pH-Responsive Release of Doxorubicin from a Mesoporous Silica-Based Nanocarrier. *Chem.—Eur. J.* **2011**, *17*, 3338–3342.

4. Sun, T. L.; Feng, L.; Gao, X. F.; Jiang, L. Bioinspired Surfaces with Special Wettability. *Acc. Chem. Res.* **2005**, *38*, 644–652.

5. Piperberg, G.; Wilner, O.; Yehezkeli, O.; Tel-Vered, R.; Willner, I. Control of Bioelectrocatalytic Transformations on DNA Scaffolds. *J. Am. Chem. Soc.* **2009**, *131*, 8724–8725.

6. Liu, T.; Yin, Y. S.; Chen, S. G.; Chang, X. T.; Cheng, S. Super-Hydrophobic Surfaces Improve Corrosion Resistance of Copper in Seawater. *Electrochim. Acta* **2007**, *52*, 3709–3713.

7. Riskin, M.; Basnar, B.; Chegel, V. I.; Katz, E.; Willner, I.; Shi, F.; Zhang, X. Switchable Surface Properties through the Electrochemical or Biocatalytic Generation of Ag^0 Nanoclusters on Monolayer-Functionalized Electrodes. *J. Am. Chem. Soc.* **2006**, *128*, 1253–1260.

8. Vlassiouk, I.; Park, C. D.; Vail, S. A.; Gust, D.; Smirnov, S. Control of Nanopore Wetting by a Photochromic Spiropyran: A Light-Controlled Valve and Electrical Switch. *Nano Lett.* **2006**, *6*, 1013–1017.

9. Kozlowskaya, V.; Kharlampieva, E.; Khanal, B. P.; Manna, P.; Zubarev, E. R.; Tsukruk, V. V. Ultrathin Layer-by-Layer Hydrogels with Incorporated Gold Nanorods as pH-Sensitive Optical Materials. *Chem. Mater.* **2008**, *20*, 7474–7485.

10. Sun, T. L.; Wang, G. J.; Feng, L.; Liu, B. Q.; Ma, Y. M.; Jiang, L.; Zhu, D. B. Reversible Switching between Superhydrophilicity and Superhydrophobicity. *Angew. Chem., Int. Ed.* **2004**, *43*, 357–360.

11. Riskin, M.; Basnar, B.; Huang, Y.; Willner, I. Magnetoswitchable Charge Transport and Bioelectrocatalysis Using Maghemite—Au Core—Shell Nanoparticle/Polyaniline Composites. *Adv. Mater.* **2007**, *19*, 2691–2695.

12. Lee, D.; Nolte, A. J.; Kunz, A. L.; Rubner, M. F.; Cohen, R. E. pH-Induced Hysteretic Gating of Track-Etched Polycarbonate Membranes: Swelling/Deswelling Behavior of Polyelectrolyte Multilayers in Confined Geometry. *J. Am. Chem. Soc.* **2006**, *128*, 8521–8529.

13. Takeuchi, T.; Goto, D.; Shinmori, H. Protein Profiling by Protein Imprinted Polymer Array. *Analyst* **2007**, *132*, 101–103.

14. Riskin, M.; Tel-Vered, R.; Bourenko, T.; Granot, E.; Willner, I. Imprinting of Molecular Recognition Sites through Electropolymerization of Functionalized Au Nanoparticles: Development of an Electrochemical TNT Sensor Based on π-Donor—Acceptor Interactions. *J. Am. Chem. Soc.* **2008**, *130*, 9726–9733.

15. Riskin, M.; Tel-Vered, R.; Frasconi, M.; Yavo, N.; Willner, I. Stereoselective and Chiroselective Surface Plasmon Resonance (SPR) Analysis of Amino Acids by Molecularly Imprinted Au-Nanoparticle Composites. *Chem.—Eur. J.* **2010**, *16*, 7114–7120.

16. Riskin, M.; Tel-Vered, R.; Lioubashevsky, O.; Willner, I. Ultrasensitive Surface Plasmon Resonance Detection of Trinitrotoluene by a Bis-Aniline-Cross-Linked Au Nanoparticles Composite. *J. Am. Chem. Soc.* **2009**, *131*, 7368–7378.

17. Riskin, M.; Tel-Vered, R.; Willner, I. Imprinted Au-Nanoparticle Composites for the Ultrasensitive Surface Plasmon Resonance Detection of Hexahydro-1,3,5-trinitro-1,3,5-triazine (RDX). *Adv. Mater.* **2010**, *22*, 1387–1391.

18. Riskin, M.; Ben-Amram, Y.; Tel-Vered, R.; Chegel, V.; Almog, J.; Willner, I. Molecularly Imprinted Au Nanoparticles Composites on Au Surfaces for the Surface Plasmon Resonance Detection of Pentaerythritol Tetranitrate, Nitroglycerin, and Ethylene Glycol Dinitrate. *Anal. Chem.* **2011**, *83*, 3082–3088.

19. Ben-Amram, Y.; Riskin, M.; Willner, I. Selective and Enantioselective Analysis of Mono- and Disaccharides Using

Surface Plasmon Resonance Spectroscopy and Imprinted Boronic Acid-Functionalized Au Nanoparticle Composites. *Analyst* **2010**, *135*, 2952–2959.

20. Frasconi, M.; Tel-Vered, R.; Riskin, M.; Willner, I. Surface Plasmon Resonance Analysis of Antibiotics Using Imprinted Boronic Acid-Functionalized Au Nanoparticle Composites. *Anal. Chem.* **2010**, *82*, 2512–2519.

21. Balogh, D.; Tel-Vered, R.; Freeman, R.; Willner, I. Photochemically and Electrochemically Triggered Au Nanoparticles "Sponges. *J. Am. Chem. Soc.* **2011**, *133*, 6533–6536.

22. Frasconi, M.; Tel-Vered, R.; Riskin, M.; Willner, I. Electrified Selective "Sponges" Made of Au Nanoparticles. *J. Am. Chem. Soc.* **2010**, *132*, 9373–9382.

23. Balogh, D.; Tel-Vered, R.; Riskin, M.; Willner, I. Electrified Au Nanoparticle Sponges with Controlled Hydrophilic/Hydrophobic Properties. *ACS Nano* **2011**, *5*, 299–306.

24. Qin, B.; Yao, R.; Zhao, X.; Tian, H. Enhanced Photochromism of 1,2-Dithienylcyclopentene Complexes with Metal Ion. *Org. Biomol. Chem.* **2003**, *1*, 2187–2191.